

## 4.4 New Instruments and Techniques

### 4.4.1 Introduction

The development of beamline instrumentation and techniques that demonstrate and enhance the unique opportunities that are available at the APS is undertaken primarily by XFD scientists and engineers on the SRI-CAT beamlines. Specifically, the goals of the SRI-CAT are:

- To develop and diagnose IDs, high heat load optics, and other novel x-ray optical components and to develop innovative techniques that will prove beneficial to the entire community of APS CATs.
- To develop and implement strategic instrumentation programs that will open up new areas of research at the APS and to extend the synchrotron radiation community beyond the current boundaries.

Some of the beamlines of SRI-CAT have been designed with flexibility in mind for the testing of beamline components and optics, while other have been designed with specific instrumentation to carry out selected areas of technique development. The later types are called strategic instruments. We currently have four strategic instruments on the Sector 2 and 3 ID beamlines:

- an instrument with milli-eV resolution
- an instrument with micro-to-nano-eV resolution to perform nuclear resonant scattering experiments

- a 1-4 keV radiation source and instrumentation for use of coherent soft x-rays
- instrumentation for development of hard x-ray microfocusing optics and techniques

A schematic of the locations of these programs, along with the other major programs, on the SRI-CAT beamlines is shown in Fig. 4.45. As indicated in the figure, SRI-CAT currently has developed five beamlines, three ID lines and two BM lines. The beamlines are made up of XFD-designed standard beamline components, whose designs are available to APS users. The SRI-CAT scientists have not only set the technical specifications for those standard components but have also commissioned them and evaluated their performance after installation

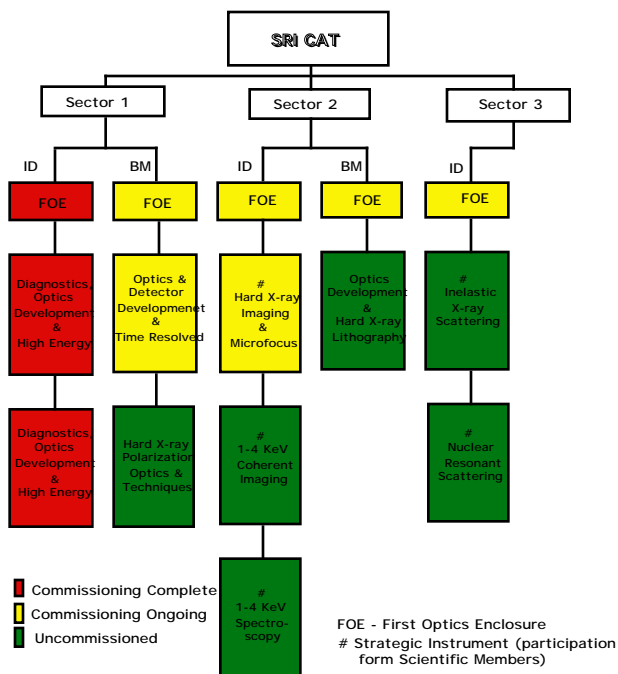


Fig. 4.45 Schematic of SRI-CAT showing activities and locations of various programs on the five beamlines.

on the beamline. The commissioning and debugging of the standard components is a valuable service to all APS users because it should allow their beamlines to come on-line in a faster and more efficient manner. Schematics of the various beamlines and their capabilities are given below along with some of the representative science that has been performed to date.

#### 4.4.2 Sector 1

Sector 1 of SRI-CAT comprises an ID beamline (1-ID) and a BM beamline (1-BM). Associated with these two beamlines are four scientific programs:

- development and characterization of high heat load optics and FE/beamline components (1-ID)
- high energy x-ray instrumentation and experimental techniques (1-ID)
- optics and techniques for time-resolved x-ray studies (1-BM-B)
- intation and techniques for the production and analysis of polarized radiation above 5 keV (1-BM-C)

Although a “home” station or beamline is indicated next to each of these programs, experiments from all four programs are carried out on both beamlines to take advantage of the different characteristics of 1-ID and 1-BM. Work on high heat load optics and FE/beamline components is described elsewhere in this document.

### 1-ID Description

The 1-ID beamline is a flexible, general purpose ID beamline that can be used for a wide variety of experiments and is particularly well suited as a test bed for novel x-ray optics. It has three stations (an FOE and two experiment stations). The 1-ID beamline was the first ID beamline to receive beam at the APS and was the first beamline to have all of its stations become operational.

The 5-meter-long straight section for the beamline has room for two IDs that can be alternatively operated. Currently, a standard APS undulator A is installed, with plans to add an APS wiggler A in the latter part of 1997. Undulator A is the most commonly used ID at the APS and produces a highly brilliant source of x-rays that can be tuned to any energy from 3.5 keV to over 200 keV. It is well suited for experiments and optics development in the x-ray energy range (6 keV to 18 keV) and also proves to be a superb source for high-energy (>50 keV) experiments.

The FOE, 1-ID-A, covers the area of the beamline immediately downstream of the ratchet-wall penetration and is used to house various components that manipulate the x-ray beam prior to transmitting the beam downstream to the experiment stations. The components in the FOE are permanent parts of the beamline and, normally, remain in place when changing to a new experiment. Among the FOE components are filters, white-beam slits, the Kohzu DCM, monochromatic-beam shutters, and a bremsstrahlung collimator/stop. A beryllium window separates the FOE portion of the beamline from the FE (i.e., the beamline inside the ratchet wall) and, hence, the storage-ring vacuum.

The 1-ID-B station is located directly downstream of 1-ID-A. Experimental equipment in 1-ID-B is mobile and can be swapped in and out depending upon the experiment. A photon/bremsstrahlung stop and a second monochromatic-beam shutter are located at the downstream end of 1-ID-B. This stop is the farthest point downstream that white beam can reach on the beamline. The 1-ID-C station is a large (4 m × 7 m) monochromatic experiment station located at the downstream end of the 1-ID beamline. As in 1-ID-B, the experimental equipment (which includes a Huber 5020 diffractometer) can be swapped in and out depending upon the experiment.

The optical concept for the 1-ID beamline is one of the simplest at the APS. In “mono-beam” mode, the white beam from the ID enters the FOE, is monochromated in the Kohzu DCM, and is then used in either 1-ID-B or 1-ID-C for experiments. In “white-beam” mode, the white beam is passed through the Kohzu DCM into the 1-ID-B station. The beam can then be used directly in 1-ID-B, or monochromated by a temporary monochromator and passed to the 1-ID-C station. Table 4.5 summarizes the hardware on 1-ID, and Fig. 4.46 shows the beamline layout.

## 1-BM Description

The 1-BM beamline has a layout similar to 1-ID in that there are three stations in tandem (1-BM-A, 1-BM-B, and 1-BM-C), but it differs considerably in optical design. The 1-BM-A station is a FOE and houses the filters, white-beam slits, collimating mirror, DCM, monochromatic-beam shutters, and bremsstrahlung collimator/stop. A beryllium window separates the FOE portion of the beamline from the FE. The 1-BM-B is an

experiment station capable of operating with white beam, “pink” beam, or monochromatic beam. The bent-crystal monochromator (BCM) is located at the upstream end of 1-BM-B and a bremsstrahlung stop is located at the downstream end of 1-BM-B. The 1-BM-C station is the end station on the beamline and accepts only monochromatic radiation. A vertically focusing mirror, monochromatic slits, and monochromatic shutter are located between 1-BM-B and 1-BM-C. The 1-BM beamline was the first BM beamline at the APS to receive beam. There are four major optical components on the 1-BM beamline:

- collimating white-beam mirror
- DCM
- BCM
- focusing monochromatic-beam mirror

The collimating white-beam mirror is 1.2 m long and made from silicon. It is water cooled and coated with palladium. This vertically deflecting, cylindrical mirror has an adjustable radius, which collimates the beam and at the same time provides harmonic rejection and power filtering. It is possible to lower the mirror out of the beam to allow the white beam onto the DCM or into 1-BM-B.

The collimating mirror is followed by the DCM, which operates between 6 keV and 25 keV using Si (111) reflections. The second crystal in the DCM is a sagittally bent crystal, which provides horizontal focusing of the beam into 1-BM-C. The crystals in the DCM can easily be removed from the beam to allow white or pink beam into 1-BM-B.

**Table 4.5 Sector 1, Insertion Device Beamline (1-ID)**

<b>Responsible Scientists</b> Dean Haeffner, phone: 630 252-0126, fax: 630 252-0161, e-mail: haeffner@aps.anl.gov Wah Keat Lee, phone: 630 252-7759, fax: 630 252-3222, e-mail: wklee@aps.anl.gov			
<b>Scientific Programs</b> <ul style="list-style-type: none"> <li>Development and characterization of high-heat-load optics and front-end/beamline components</li> <li>High-energy x-ray instrumentation and experimental techniques</li> </ul>			
<b>Source Characteristics</b> <ul style="list-style-type: none"> <li>APS Undulator A (operational)</li> <li>APS Wiggler A (not yet installed)</li> </ul>			
<b>Optical Components</b>			
Component	Distance from Source (m)	Description	Status
White beam slits (L5)	28.0	Horiz. & vert.	Operational
Kohzu double crystal mono.	29.8	LN <sub>2</sub> cooled Si or diamond	Operational
Mono slits (L2)	37.8	Horiz. & vert.	Operational
<b>Beamline Configurations (1-BM)</b> <ul style="list-style-type: none"> <li>Monochromatic beam into B &amp; C</li> <li>White beam into B, monochromatic beam into C</li> </ul>			
<b>Detectors</b> <ul style="list-style-type: none"> <li>NaI scintillation counters</li> <li>Ionization chambers</li> <li>Ge and Si solid state</li> </ul>			
<b>Beamline Control</b> <ul style="list-style-type: none"> <li>UNIX-based Sun workstations</li> <li>VME</li> <li>EPICS</li> <li>SPEC</li> </ul>			
<b>Ancillary Equipment</b> <ul style="list-style-type: none"> <li>Huber D5020 4-circle diffractometer on motorized table</li> <li>Motorized optical tables</li> <li>LN<sub>2</sub> pump</li> </ul>			

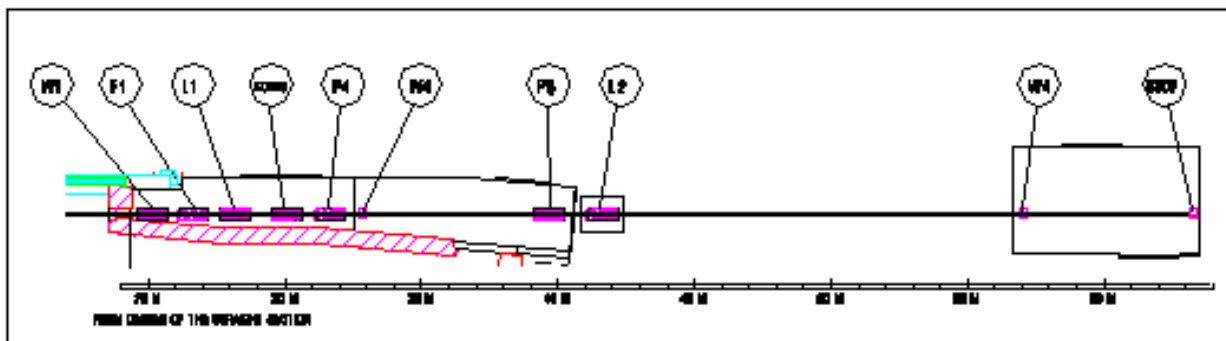


Fig. 4.46 Schematic layout of the Sector 1 ID beamline. Beam enters from the left and travels to the right. W1: beryllium window, F1: filter, L1: white-beam slits, KOHZU: double-crystal monochromator, P4: moveable white-beam stop and monochromatic shutter, W4: beryllium window, P5: fixed white-beam stop and monochromatic shutter, L2: monochromatic-beam slits, W5: beryllium window.

The BCM is located at the upstream end of 1-BM-B and can only deliver beam within this station. This monochromator uses a four-point bender with a single crystal (typically Si (220)) to meridionally focus the beam. The BCM provides a polychromatic horizontal focus with a spot size of  $\sim 150 \mu\text{m}$  and a bandpass up to 1 keV. Its primary use is for energy-dispersive experiments. When the DCM is being used, the crystal in the BCM may be removed from the beam.

The second mirror is 1 m long and made from silicon. Like the first mirror, it is a palladium-coated, vertically deflecting cylindrical mirror with an adjustable radius. This mirror provides vertical focusing of the beam from the DCM into 1-BM-C. Table 4.6 summarizes the hardware on 1-BM, and Fig. 4.47 shows a beamline layout.

### Current Status

All components for undulator operation have been installed and commissioned on the 1-ID beamline. For wiggler operation, some components will require alterations and those

changes are expected to be completed in calendar year 1997. When the monochromatic mirror is installed in the fall of 1997, the 1-BM line will then be fully operational.

### High Energy X-ray Instrumentation and Techniques

The goal of the high energy x-ray program is to develop instrumentation and techniques that utilize the abundant potential of the APS as a source of photons in the 30 keV to 200 keV range. The initial efforts to meet the wide scope of this goal have been to characterize the high energy x-rays from undulator A, measure the scattering from several liquid or amorphous materials for comparison to neutron data, and to characterize optics for high resolution Compton scattering.

A series of experiments were carried out to characterize the performance of the APS undulator A for delivering photons above 50 keV. The measured spectra from several different undulator gaps are shown in Fig. 4.48. The size of the monochromatic



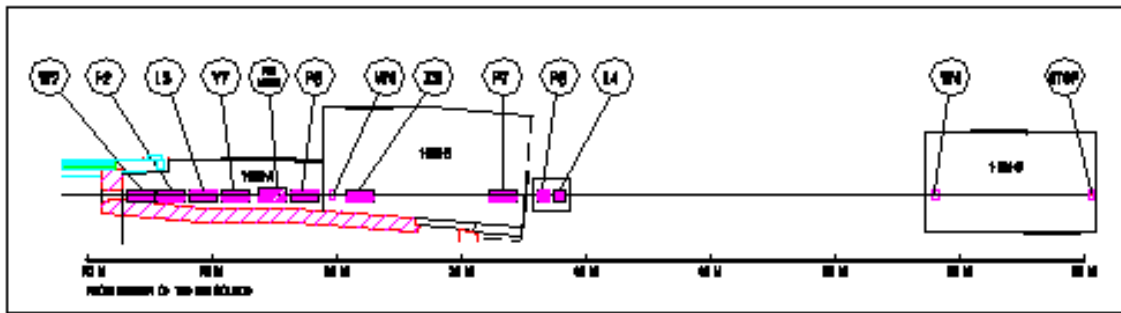


Fig. 4.47 Schematic layout of the Sector 1 BM beamline. Beam is traveling left to right. W2: beryllium window, F2: filter, L3: white-beam slits, Y7: collimating mirror, PSL MONO: double-crystal monochromator, P6: movable white-beam stop and monochromatic shutter, W4: beryllium window, X3: bent-crystal monochromator, P7: white-beam stop and monochromatic shutter, P8: monochromatic shutter, L4: monochromatic slits, W4: beryllium window.

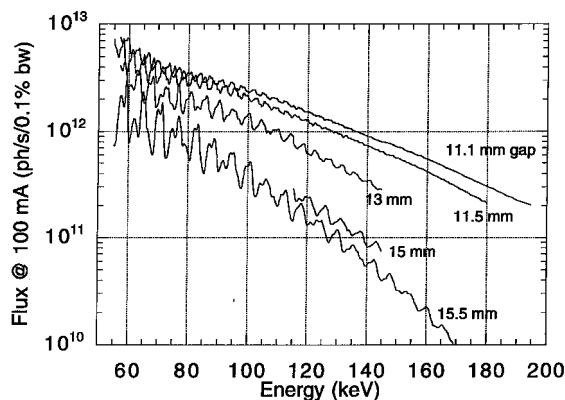


Fig. 4.48 APS undulator on-axis flux spectra through a 1 mm  $\times$  1 mm aperture located 35 meters from the source.

beam was also measured for several energies at various undulator gaps. These results agree well with calculations made using the UR computer code (developed at the APS). Code UR uses the measured magnetic fields from actual devices in generating photon spectra. From the measurements it was found that undulator structure can be seen out to the 35th harmonic and that at high energies the performance of the undulator approaches that of a low-K wiggler.

Among the characteristics that differentiate “high energy” x-rays from photons in the more commonly used x-ray energy range (6 keV to 20 keV) is much lower absorption by materials and smaller diffraction angles for equivalent momentum transfer. Both of these attributes are utilized in the study of x-ray scattering from amorphous/liquid materials. The absorption is comparable to that of neutrons for many materials, allowing the same samples and geometries to be used in both x-ray and neutron studies. This greatly simplifies the task of comparing x-ray and neutron results for materials for which “near-surface” effects are at issue. The low absorption also makes possible the study of materials inside relatively heavy containers (e.g., corrosive materials in stainless steel or samples at extreme temperatures and pressures). The small angles allow for the measurement of momentum transfer out to very large  $Q$  (up to 20  $\text{\AA}^{-1}$ ), which is needed for accurate structural determination.

A collaboration has been started with ANL/Materials Science Division scientists to use high energy x-rays to examine amorphous glasses or liquids that have previously been

studied with neutrons, but are difficult (if not impossible) to study with “ordinary” x-rays. The first experiments have used 50 keV and 150 keV x-rays from 1-BM to examine molten  $\text{FeCl}_3$ , molten KPb, and  $\text{GeO}_2$  glass. For these experiments, the  $\text{FeCl}_3$  was contained in a tube of  $\text{SiO}_2$  and heated to 600 K, and the KPb was in a vanadium can (as was used for neutron experiments) and heated to 800 K. The normalized data for molten  $\text{FeCl}_3$  taken with both the neutrons and high energy x-rays are shown in Fig. 4.49. Because the ratio of scattering from Fe to that from Cl is higher for x-rays than for neutrons, it is quite easy to see that the second peak has more of a Cl contribution than the third peak. From detailed analysis, quantitative information is obtained about the partial structure factors.

Another aspect of the high energy program is to develop optics for high resolution Compton scattering. As part of this effort, a cryo-cooled DCM using Si (111) crystals set to diffract 86 keV was assembled and put into 1-ID-B (86 keV is well outside the operating range of the Kohzu DCM). The monochromatic beam was then delivered to 1-ID-C to allow for data collection with very low background

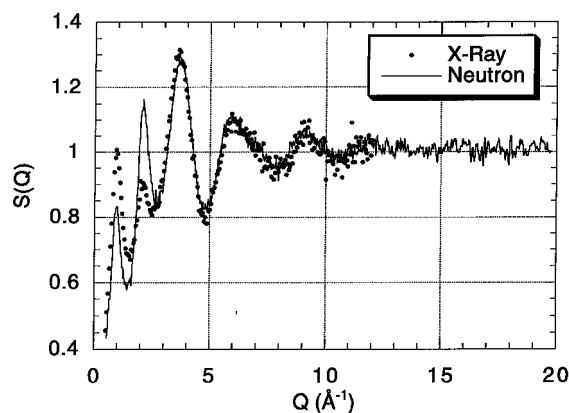


Fig. 4.49 Comparison of the scattering from molten  $\text{FeCl}_3$  at 600 K for 50 keV x-rays and neutrons.

radiation. This beam was used to characterize both a scanning Laue analyzer and a Cauchois-type analyzer (used with image plates). Resolutions of approximately 0.1 a.u. were obtained for both systems. The next step in this effort will be to adapt the monochromator crystals to a bent Laue-Bragg system to increase throughput and focus the beam.

### Hard X-ray Polarization Program

The main objective of the hard x-ray polarization program is the development of instrumentation and techniques for the production and analysis of polarized synchrotron radiation. Particular emphasis has been given to the design of phase-retarding crystal optics that yield the following characteristics:

- high degree of circular polarization
- high degree of stability
- tunability in a wide energy range
- rapid helicity switching

To accomplish this, phase retarders have been developed for two energy regimes: low energies (5 keV–30 keV) and high energies (>30 keV). For low energies, helicity-switching phase retarders made of thin (50  $\mu\text{m}$  to 1000  $\mu\text{m}$ ) single-crystal diamond or silicon have been tested (see Fig. 4.50). These phase retarders are suitable for magnetic circular dichroism or resonant-magnetic-scattering experiments. For high energies, a new helicity-switching phase retarder designed to operate at 86 keV has been manufactured and



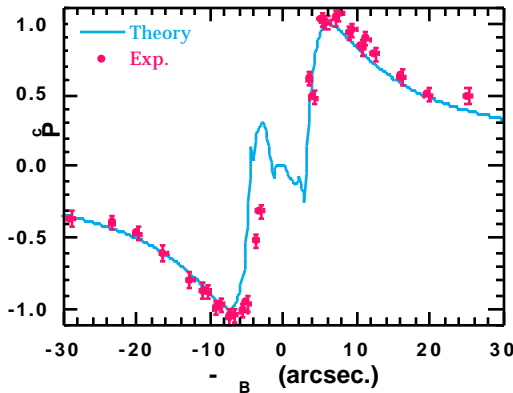


Fig. 4.50 Measured and theoretical circular polarization for the transmitted beam in a 75-mm-thick Si (400) crystal at 8.0 keV.

successfully tested (see Fig. 4.51). The high energy phase retarder is made of a single, monolithic germanium crystal in the Bragg-Laue design. With further improvements of this phase retarder in mind, work on the development of a broad (1 keV) bandpass high energy monochromator is currently in progress. These monochromators are made of W/Si bilayers with a goal of ~90% reflectivity at 100 keV. For polarization analysis, a polarimeter utilizing multibeam diffraction was built and tested. This device enables complete characterization of polarization for energies up to 15 keV.

To utilize and further test the low energy, phase-retarding optics developed at the APS, a series of temperature-dependent dichroism experiments have been performed. The goal of these experiments was to measure the different exchange couplings present in rare earth-transition metal alloys. An example of the results is shown in Fig. 4.52, which shows the temperature dependence of the dichroism in HoFe<sub>2</sub>. The different temperature dependencies of the lower negative feature and higher positive feature are directly correlated with the magnetization of the Ho 4f and 5d bands. An understanding of the exchange

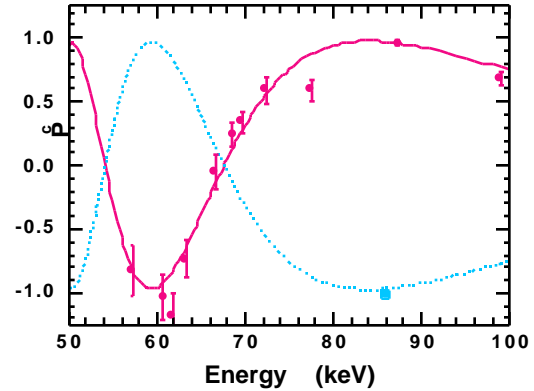


Fig. 4.51 Measured and theoretical rate of circular polarization for the (220) and (2-20) beams as a function of energy. The phase retarder is designed to operate at 86.5 keV.

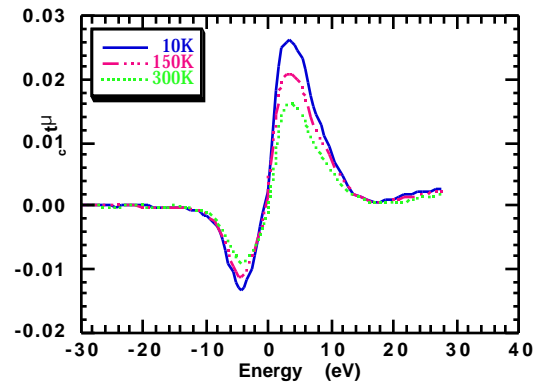


Fig. 4.52 Variations in the dichroic spectrum as a function of temperature at the Ho L<sub>3</sub> edge of HoFe<sub>2</sub>.

couplings that control the magnetization of the 5d band is essential in the development of new magnetic materials. The use of phase-retarding optics proved essential in this experiment due to the difficulty of reversing the sample magnetization in cryogenic environments.

As a continuation of the study of magnetic systems utilizing circularly polarized hard x-rays, preliminary experiments on the magnetic properties of thin films have commenced and a program exploring

spin-dependent Compton scattering has been initiated.

## Time-Resolved Studies

The primary goal of the time-resolved program is the development of instruments and techniques for time-resolved x-ray studies. The primary x-ray optic associated with the time-resolved program is the dispersive BCM located in the 1-BM-B station. The BCM provides a polychromatic beam with a distinct relation between angle and beam energy such that when used with spatially resolved detectors (see below), time-resolved EXAFS or dispersive-diffraction spectra can be collected. The BCM has been designed to operate in an energy range between 6 and 20 keV, typical for absorption edges of interest in EXAFS studies. The horizontal spot size produced by the BCM has been measured to be ~150 microns at 11.0 keV with a measured flux of  $1.5 \times 10^{11}$  ph/s/100 mA.

An integral part of the time-resolved program is the development of high speed area detectors. For time-resolved x-ray scattering, charge coupled device (CCD) detectors with multiple outputs are the best choice for high speed, reasonable-size applications. Current commercially available detectors have frame rates comparable to that of TV signaling rates, 30 frames per second (fps). Typically these cameras can digitize each pixel at up to 10 bits (1024 light levels). At slower frame rates (typically less than 1 fps), it is possible to digitize each pixel to 16 bits. These cameras are not adequate for the types of experiments we envision for the APS, hence we have pursued a program for the development of a high framing rate CCD-based camera system.

The camera system that has been developed here is composed of a camera head unit and a data collection unit. The camera head unit uses a CCD as the x-ray imager. It contains all of the circuitry necessary to control the CCD and digitize each pixel. The data collection unit consists of a digital interface capable of storing high speed digital data. The camera was designed for a multiple output CCD with a maximum pixel rate of 20 MHz per output. This gives a 2-output CCD with an area of  $512 \times 512$  pixels a readout time of about 10 milliseconds (ms), corresponding to a maximum of about 100 fps. The camera digitizes each pixel to 12 bits (one of 4096 light levels). The data rate from this camera will be up to 80 megabytes per second. The data collection unit must capture and store this data. The approach used is to store the data in an intermediate storage area before they are written to a disk drive of a computer so that they can be manipulated, analyzed, and permanently archived. This intermediate storage area is conventional dynamic random access memory (DRAM). The acquisition unit can be designed in two ways. The data can be written directly to a DRAM storage card and then read out to a computer and stored to a hard disk drive. For time-resolved x-ray imaging, the camera is used with a phosphor screen to convert x-ray photons to visible light that is then imaged onto the CCD. This imaging is either done by lenses (for large area imaging) or by means of a fiber-optic face plate or taper directly bonded to the CCD. The phosphor screen in this case is coupled by means of optical gel to the fiber-optic element. The camera is designed so that it can also be used as a streak camera where one or several rows of data are read out continuously achieving time resolutions of few tens of microsecond. The camera system has been also tested using a  $1024 \times 1024$  pixel CCD from Texas Instruments (TC215) that is read out from two outputs as a  $512 \times 512$  device.

with four pixel hardware binning. A camera currently being designed is based upon a Thomson TH7896 ( $1024 \times 1024$ , 4 output). After the engineering issues of a 4-output camera are solved, a camera will be developed using a 16-output  $512 \times 512$  Sarnoff CCD capable of 800 frames/second.

To date, the camera system has been used as a diagnostic tool in the commissioning of the dispersive monochromator on the 1-BM beamline. The camera system was used to collect the Cu absorption spectrum in 10 milliseconds (shown in Fig. 4.53) and has been configured to be used as a streak camera, measuring the absorption of copper with a time resolution of 50 microseconds.

#### 4.4.3 Sector 2

Sector 2 consists of an ID beamline (2-ID) with three branches and a BM beamline (2-BM). At Sector 2, there are five scientific programs distributed among four experiment end stations:

- High resolution microfocusing and microscopy (2-ID-B, 2-ID-D)
- Coherence and correlation techniques (2-ID-B, 2-ID-D)
- High resolution spectroscopy and polarization physics (2-ID-C)
- X-ray optics characterization and technique development (2-BM-B)
- Deep x-ray lithography (2-BM-B)

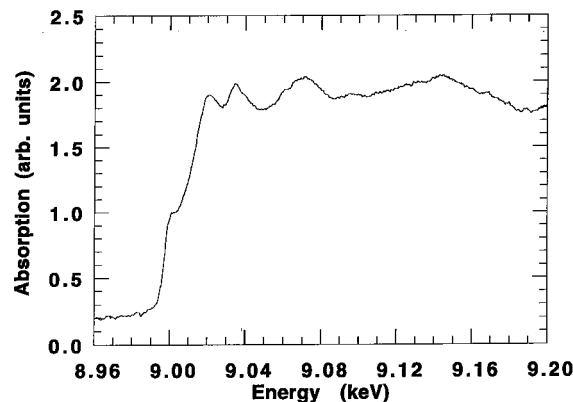


Fig. 4.53 Cu EXAFS spectrum taken in 10 ms using the dispersive monochromator.

### Beamline Descriptions

To accomplish the objectives of the Sector 2 scientific programs, the first- and third-order harmonics of two 2.4-m-long undulators (a standard 3.3-cm-period APS undulator A and a special 5.5-cm-period undulator) are used to cover the 0.5-32 keV x-ray energy range on the 2-ID beamline. The 2-BM source has a critical energy of 19.5 keV and provides broadband x-rays over the 0.5-32 keV region. Details of the source, optics, and beamline design can be found in the Sector 2 Preliminary Design Report, Final Design Report, and elsewhere (Yun et al., 1996a, 1996b; Shu et al., 1996; McNulty et al., 1996; Lai et al., 1996). A brief description is given here.

#### 2-ID

The 2-ID-A station FOE houses various apertures and optics to handle the high incident power and manipulate the incident x-ray beam. The three branch lines share the FOE but have independent experiment

stations, 2-ID-B, 2-ID-C, 2-ID-D/E (see Fig. 4.54). The three branch lines also share a water-cooled, high heat load, horizontally deflecting mirror (M1) that operates at a grazing incidence angle of  $0.15^\circ$ . The pink beam following M1 has a maximum cutoff energy of 32 keV. The branching is achieved inside 2-ID-A using horizontally deflecting mirrors: a second mirror (M2B or M2C, depending on the branch line in operation), and a third mirror (M3B). The other components in 2-ID-A include a fixed aperture, an adjustable aperture, a bremsstrahlung collimator, a white-beam stop, a BPM, and beam shutters for each branch line. These components are permanent parts of the beamline that remain in place when switching between branch lines.

The 2-ID-B branch line is designed for the 0.5-4 keV energy range. It receives the beam

reflected successively by the M1, M2B, and M3B mirrors and is oriented at an angle of  $5.0^\circ$  to the 2-ID-D/E branch. Branch line 2-ID-B uses a horizontally deflecting spherical grating monochromator (SGM) consisting of an entrance slit, a grating chamber holding up to five diffraction gratings, an exit slit, a differential pump, and a silicon nitride exit window inside an environmentally isolated experimental enclosure. The enclosure provides acoustic and temperature control for sensitive experiments. The branch line has three BPMs for beam monitoring and feedback.

The 2-ID-C branch line operates over the 0.5-3 keV range. It receives the beam reflected successively by the M1 and M2C mirrors at an angle of  $2.5^\circ$  to the 2-ID-D/E branch. Branch line 2-ID-C has a vertically deflecting third mirror (M3C, located outside of 2-ID-A) for

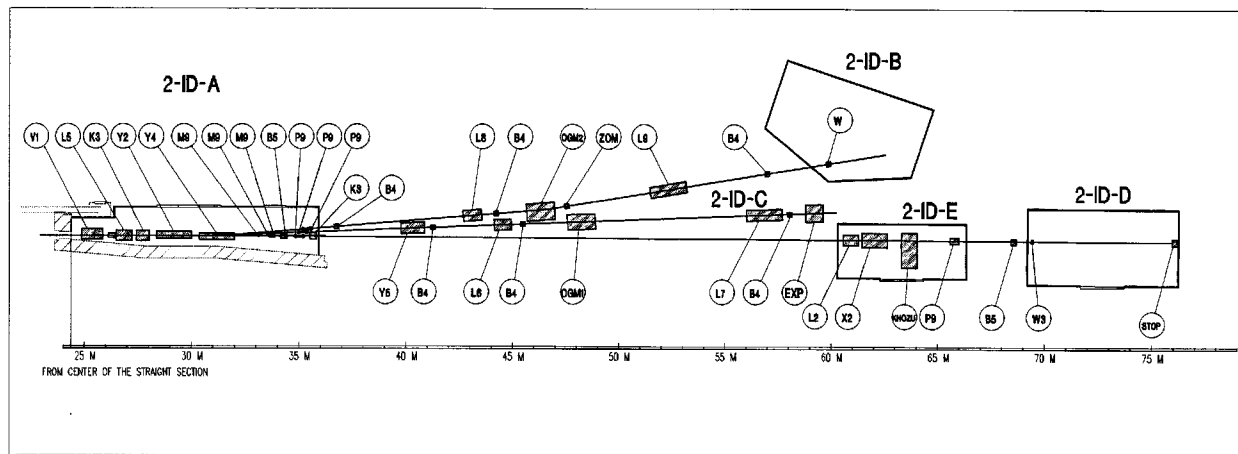


Fig. 4.54 Schematic of beamline 2-ID. The labeled components in 2-ID-A are: V1, differential pump and cooled aperture; L5, adjustable slits; K3, bremsstrahlung collimator; Y2, high heat load horizontally deflecting mirror (M1); Y4, soft x-ray horizontally deflecting beam-branching mirrors (M2C, M2B, M3B); M9, cooled masks; B5, beam position monitor; P9, branch line shutters; K3, collimator. The branch line and experiment station components are: B4, beam position monitor; Y5, vertically focusing mirror; L6 and L8, entrance slits; L7 and L9, exit slits, OGM1, vertically deflecting SGM; OGM2, horizontally deflecting SGM; ZOM, zero-order mask; W, silicon nitride window; EXP, soft x-ray spectroscopy station; L2, adjustable slits; X2, double-multilayer monochromator; Kohzu, DCM; P9, shutter; B5, beam position monitor; W3, beryllium window; STOP, beam stop.

vertical focusing. Mirror M3C deflects the beam downward by  $2^\circ$ . The 2-ID-C branch line uses a vertically deflecting SGM optimized for high spectral resolution. The experiment station following the exit slit consists of a UHV experimental chamber. Branch line 2-ID-C also has three BPMs.

The 2-ID-D/E branch line is designed to cover 4-32 keV and has two experiment stations, 2-ID-E and 2-ID-D. The 2-ID-E station is located at  $\sim 30$  m downstream of 2-ID-A and houses pink-beam slits, a double-multilayer monochromator, a beryllium window, a DCM, and a pink-beam shutter. The main experiment station, 2-ID-D, can receive pink or monochromatic beam through a final beryllium window.

The three branch lines cannot be operated simultaneously in the current design. However, switching of the beam from one branch to another can be completed in a few minutes. A significant portion of the experiments planned for the branch lines may

be performed with little compromise by beam sharing. A summary of the beamline hardware is shown in Tables 4.7, 4.8, and 4.9.

## 2-BM

The 2-BM beamline has two experiment stations, 2-BM-A and 2-BM-B (see Fig. 4.55). Station 2-BM-A (which is also serves as a FOE) contains a mirror and two monochromators to satisfy the different bandwidth requirements of the experimental program. A DCM is used for experiments requiring narrow band x-rays, whereas a double-multilayer monochromator provides broad band monochromatization. The other components in 2-BM-A include a fixed mask, differential pumping station, filter assembly, white-beam slits, bremsstrahlung collimator, beryllium window, and a shutter.

The 2-BM-B station is located  $\sim 20$  m further downstream. It can receive either the monochromatic or pink beam from 2-BM-A. It

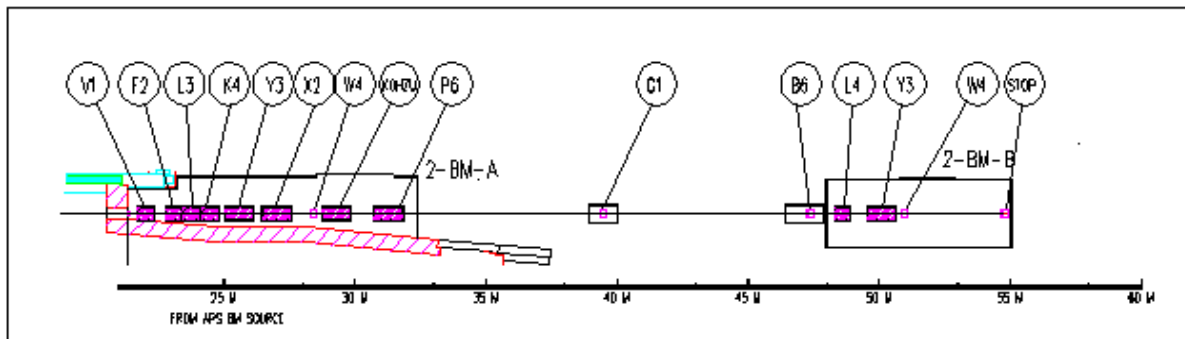


Fig. 4.55 Schematic of beamline 2-BM. The components in 2-BM-A are: V1, differential pump and cooled aperture; F2, selectable filters; L3, adjustable slits; K4, bremsstrahlung collimator; Y3, vertically deflecting mirror (M1); X2, double-multilayer monochromator; W4, beryllium window; Kohzu, DCM; P6, shutter. Following 2-BM-A are: G1, diagnostic screen; B6, beam position monitor; L4, adjustable slits; Y3, vertically deflecting mirror (M2) W4, beryllium window; STOP, beam stop.

**Table 4.7 Sector 2, Insertion Device Branch Line (2-ID-B)**

<b>Responsible Scientists</b> Ian McNulty, phone: (630) 252-2882, fax: (630) 252-9303, e-mail: mcnulty@aps.anl.gov Yiping Feng, phone: (630) 252-1081, fax: (630) 252-9303, e-mail: yfeng@aps.anl.gov			
<b>Scientific Programs</b> <ul style="list-style-type: none"><li>• High resolution imaging</li><li>• Coherent scattering</li><li>• Interferometry</li></ul>			
<b>Source Characteristics</b>			
<b>Undulator</b>			
Length	2.47 m		
Periods	44, 5.5 cm		
Kmax	5.6		
Peak power density	134 kW/mrad <sup>2</sup>		
Energy range	0.5-7.0 keV in the first harmonic		
Spectral flux	10 <sup>13</sup> -10 <sup>15</sup> ph/s/0.1% BW		
Coherent flux	10 <sup>10</sup> -10 <sup>12</sup> ph/s/0.1% BW		
<b>Optical Components</b>			
Component	Distance from Source (m)	Description	Date Available
Horiz. and vert. slits	27.0	25 μm reproducibility	04/1997
Mirror (M1)	29.5	0.15 degree plane (Pt) high heat load	07/1996
Mirror (M2B)	30.6	1.25 degree sphere, horiz. focussing	06/1997
Mirror (M3B)	41.4	1.25 degree sphere, vert. focussing	06/1997
Monochromator	50.0	Multilayer spherical grating	06/1997
Microprobe	60.0	Zone plate	10/1997
<b>Beamline Characteristics</b>			
Energy range	0.5-4.0 keV		
Monochromaticity	10 <sup>2</sup> -10 <sup>4</sup> E/dE		
Beam size	2.0 × 0.5 mm <sup>2</sup> (horiz. × vert.)		
Microprobe focus size	0.1 × 0.1 μm <sup>2</sup> (horiz. × vert.)		
Microprobe flux	10 <sup>6</sup> -10 <sup>8</sup> ph/s/0.1% BW		
<b>Detectors</b> <ul style="list-style-type: none"><li>• Ionization chambers</li><li>• Avalanche photodiodes</li><li>• Windowless dispersive LEGe</li><li>• Thinned/backside-illuminated CCD camera</li></ul>		<b>Beamline Control</b> <ul style="list-style-type: none"><li>• EPICS</li></ul>	
<b>Ancillary Equipment</b> <ul style="list-style-type: none"><li>• Scanning/holographic microscope</li><li>• 2-circle goniometer</li><li>• Image processing workstation</li></ul>			

**Table 4.8 Sector 2, Insertion Device Branch Line (2-ID-C)**

<b>Responsible Scientists</b> Kevin J. Randall, phone: (630) 252-9614, fax: (630) 252-9303, e-mail: randall@aps.anl.gov Joseph Z. Xu, phone: (630) 252-0143, fax: (630) 252-0161, e-mail: jzxu@aps.anl.gov			
<b>Scientific Programs</b> <ul style="list-style-type: none"><li>High resolution polarization-dependent spectroscopy</li></ul>			
<b>Source Characteristics</b>			
<b>Undulator</b>			
Length	2.47 m		
Periods	44, 5.5 cm		
Kmax	5.6		
Peak power density	134 kW/mrad <sup>2</sup>		
Energy range	0.5-7.0 keV in the first harmonic		
Spectral flux	10 <sup>13</sup> -10 <sup>15</sup> ph/s/0.1% BW		
Coherent flux	10 <sup>10</sup> -10 <sup>12</sup> ph/s/0.1% BW		
<b>Optical Components</b>			
Component	Distance from Source (m)	Description	Date Available
Horiz. and vert. slits	27.0	25 μm reproducibility	04/1997
Mirror (M1)	29.5	0.15 degree plane (Pt) high heat load	07/1996
Mirror (M2C)	30.6	1.25 degree sphere, horiz. focussing	06/1997
Mirror (M3C)	41.4	1.00 degree sphere, vert. focussing	10/1997
Monochromator	50.0	Multilayer spherical grating	10/1997
Experiment station	60.0	UHV sample chamber	10/1997
<b>Beamline Characteristics</b>			
Energy range	0.5-3.0 keV		
Monochromaticity	10 <sup>3</sup> -10 <sup>4</sup> E/dE		
Beam size at sample	1.0 × 1.0 mm <sup>2</sup> (horiz. × vert.)		
Flux at sample	10 <sup>11</sup> -10 <sup>13</sup> ph/s		
<b>Detectors</b> <ul style="list-style-type: none"><li>Hemispherical electron/ion analyzer</li><li>Electron spin detector</li><li>Photodiodes</li><li>Windowless Si(Li) detector</li><li>Total electron yield detector</li></ul>		<b>Beamline Control</b> <ul style="list-style-type: none"><li>EPICS</li></ul>	
<b>Ancillary Equipment</b> <ul style="list-style-type: none"><li>UHV reflectometer</li><li>UHV polarimeter</li><li>100 nm electron gun</li></ul>			

**Table 4.9 Sector 2, Insertion Device Branch Line (2-ID-D/E)**

<b>Responsible Scientists</b> Wenbing Yun, phone: (630) 252-5320, fax: (630) 252-9303, e-mail: yun@aps.anl.gov Zhonghou Cai, phone: (630) 252-0144, fax: (630) 252-0161, e-mail: cai@aps.anl.gov			
<b>Scientific Programs</b> <ul style="list-style-type: none"><li>• High resolution imaging</li><li>• Coherence-based techniques</li></ul>			
<b>Source Characteristics</b>			
<b>Undulator</b>			
Length		2.47 m	
Periods		74, 3.3 cm	
Kmax		2.6	
Peak power density		170 kW/mrad <sup>2</sup>	
Energy range		3.2-13.0 keV in the first harmonic	
Spectral flux		10 <sup>12</sup> -10 <sup>14</sup> ph/s/0.1% BW	
Coherent flux		10 <sup>10</sup> -10 <sup>12</sup> ph/s/0.1% BW	
<b>Optical Components</b>			
Component	Distance from Source (m)	Description	Date Available
Horiz. and vert. slits	27.0	25 μm reproducibility	04/1997
Mirror (M1)	29.5	0.15 degree plane (Pt) high heat load	07/1996
Double crystal mono.	62.0	Kohzu, Si (111)	12/1996
Double multilayer mono.	63.7	Medium resolution	10/1997
Microprobe	71.0	Zone plate	12/1996
<b>Beamline Characteristics</b>			
Energy range		2.0-32.0 keV	
Monochromaticity		1.0-10 <sup>4</sup> E/dE	
Beam size		4.2 × 1.6 mm <sup>2</sup> (horiz. × vert.) FWHM	
Microprobe focus size		0.1 × 0.1 μm <sup>2</sup> (horiz. × vert.)	
Microprobe flux		10 <sup>11</sup> ph/μm <sup>2</sup> /s/0.1% BW	
<b>Detectors</b> <ul style="list-style-type: none"><li>• Ionization chambers</li><li>• NaI scintillation detector</li><li>• Avalanche photodiodes</li><li>• CCD camera</li><li>• 13-element energy-dispersive detector</li></ul>		<b>Beamline Control</b> <ul style="list-style-type: none"><li>• EPICS</li></ul>	
<b>Ancillary Equipment</b> <ul style="list-style-type: none"><li>• Optical tables with 6 degrees of freedom</li><li>• Scanning microscope</li><li>• High resolution x-ray spectrometer</li><li>• Image processing workstation</li></ul>			



contains a beam position monitor, monochromatic beam slits, and a beryllium exit window. In 2-BM-B there is also a mirror that is used as a broad band energy selector. The required spectral range (e.g., for lithography experiments) can be adjusted by varying the incidence angle of the mirror. Table 4.10 provides a summary of the beamline characteristics and hardware.

### **Current status**

Construction and commissioning of Sector 2 is about 70% complete. Both experiment stations of 2-BM have been commissioned; 2-BM-A awaits a double-multilayer monochromator, the last major component to be installed in 2-BM. Most of the components in the 2-ID-A FOE and the 2-ID-D/E branch line have been commissioned. The final component to be installed in 2-ID-A is the M2C/M2B/M3B mirror manipulator and branch-line switching system. A double-multilayer monochromator and integral shutter remain to be installed in 2-ID-E, whereas the 2-ID-D station is complete. The 2-ID-B and 2-ID-C branch lines and end stations are under construction and to be commissioned in mid-1997.

### **Scientific Program**

#### **2-ID**

The main objective of the 2-ID scientific program is to develop experimental techniques and instrumentation that utilize the high spectral brilliance, large transverse coherence widths, and low energy polarization properties of the APS undulator beams. These include high resolution x-ray microfocusing,

spectroscopy, coherence, and correlation experiments. In addition to these areas, the 2-ID beamlines will be used to develop diagnostic techniques for measuring the source emittance, characterizing the absolute flux, intensity, and low energy polarization of the beam, and for developing high performance x-ray optics (mirrors, multilayers, crystals, and gratings) to preserve the brilliance and low energy polarization of the undulator beam under high heat load conditions.

#### ***High resolution microfocusing and microscopy***

The 2-ID-B and 2-ID-D/E branch lines provide undulator radiation with the spectral and coherence properties required for development of high resolution x-ray microfocusing optics and related techniques, such as scanning microscopy, phase-contrast microscopy, microdiffraction, microimaging, and microanalysis in the intermediate and high energy ranges from 0.5-4 and 4-32 keV, respectively. Consequently these branch lines are optimized for brilliance and coherence preservation, high order harmonic rejection, and angular stability.

Several experiments have been carried out since the commissioning of the 2-ID-D station in December 1996. Selected results are presented below.

(1) Study of an electro-absorption laser/modulator using x-ray microdiffraction. In collaboration with a team from Lucent Technologies, we have made spatial maps of the crystallographic strain, composition, and multiquantum well thickness of an integrated laser/modulator device, one of the key components in long-haul lightwave



transmission systems. The device is an InGaAsP-based monolithic quantum well laser and modulator, which has an active region about 1 mm wide. The microbeam is essential for mapping the strain field in a buried device with such dimensions. The strain field in the laser and modulator, and the transition region between them, has important consequences for device performance. The strain is measured by taking a Bragg scan ( $\theta/2$ ) along the growth direction and determining the position of the zeroth order quantum-well superlattice peak (Fig. 4.56). The quantum well and barrier thickness are determined from the spacing of the superlattice peaks and their

relative intensities. This information is very useful for guiding the device fabrication process.

(2) Study of the plant-fungi relationship in contaminated environments. The objective of this project is to study the relationship between plants and mycorrhizal fungi in soils contaminated by heavy metals and radionuclides. An understanding of the role of mycorrhizal fungi in the adaptation of plants to contaminated environments and the elucidation of the uptake and sequestration mechanisms for heavy metal and radionuclides in these

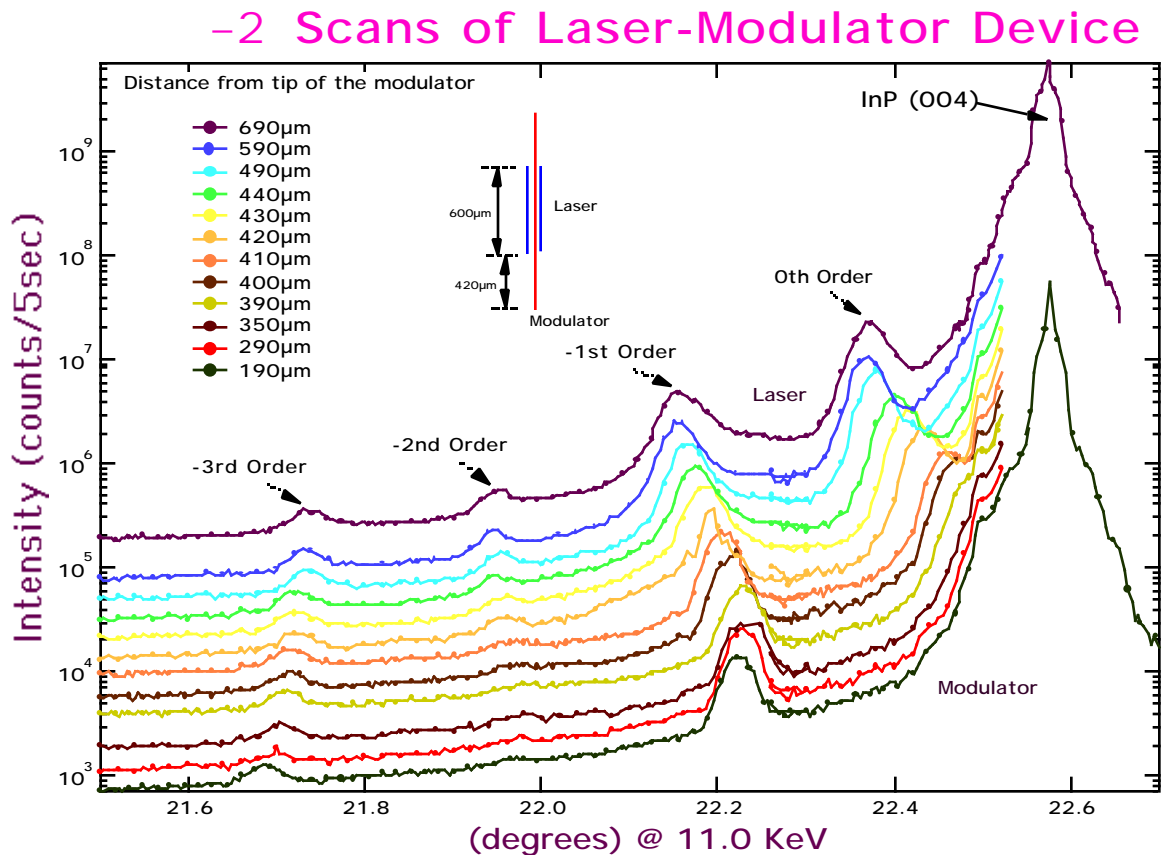


Fig. 4.56 Radial Bragg scans along the In (004) substrate direction taken at several positions. The focal spot was about  $1\ \mu\text{m}$  (V)  $\times$   $3\ \mu\text{m}$  (H). The variation in multi-quantum well period and strain as a function of position is observed as a variation in spacing between superlattice peaks (labeled by order) and position of the zeroth-order peak, respectively.

systems are expected to have important ramifications both in the remediation and restoration of waste sites and in the assessment of risk associated with such sites.

X-ray fluorescence microscopy was used for mapping elemental distributions of several metallic elements, including Ca, Cr, Fe, Zn, Cu, and K. We were able to detect trace elements in a single fungi strand with diameters of about 10  $\mu\text{m}$ . Using x-ray phase contrast imaging, we were able to record images of a single strand. With improved detector resolution and efficiency, a phase contrast microscope with 1- $\mu\text{m}$  resolution and the sensitivity to detect submicron-thick biological samples can be developed. The combination of this capability with the elemental sensitivity may prove to be an extremely useful tool for biological research.

(3) X-ray microdiffraction study of fiber-reinforced materials. Fabrication-induced residual stress in engineered composites consisting of continuous fibers may result in large tensile hoop stresses at the fiber/matrix interface, sufficient to cause plastic deformation or radial cracking of the matrix in low ductility systems. An understanding of the residual and operational stress field near the interface between the matrix and fiber is of great importance to designers of components as well as materials engineers responsible for developing processes for fabricating high quality composites.

Using x-ray microdiffraction techniques, we mapped the strain field in a composite material system consisting of SiC fibers in a Ti/Al/Nb host matrix. Preliminary analysis of the data indicates that good agreement was obtained between the measured strained field and that calculated using a simple continuum

model (Fig. 4.57). The high spatial resolution (10  $\mu\text{m}$ ) is essential for this measurement because the strain field changes rapidly over a region of 50  $\mu\text{m}$ .

### Coherence and correlation techniques

The 2-ID-B and 2-ID-D/E branch lines are also dedicated to development of x-ray coherence-based and correlation techniques such as holography, interferometry, speckle, and correlation spectroscopy. Both branch lines offer selectable energy bandwidth and spatial coherence of the beam in order to satisfy the needs of a wide variety of coherence dependent experiments.

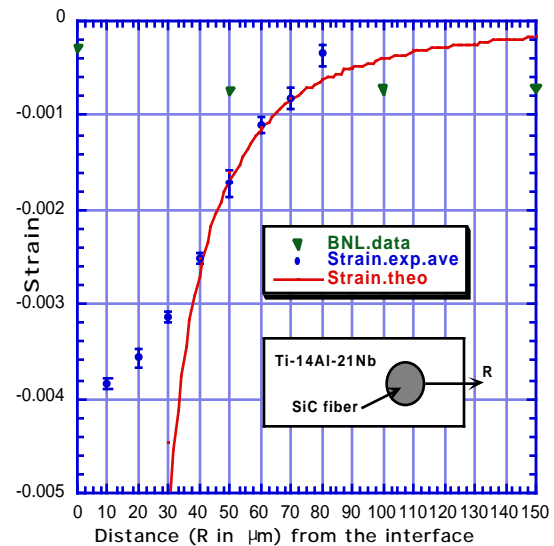
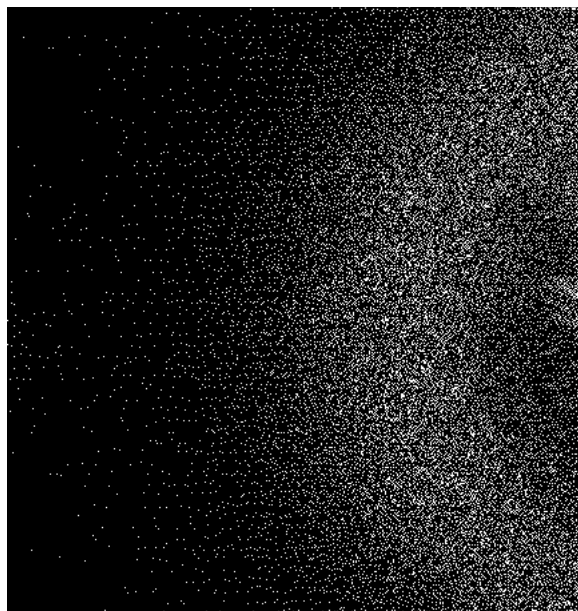


Fig. 4.57 Measured strain field using our x-ray microscope (dots) at the APS, measured strain using a 50  $\mu\text{m}$  pinhole at the NSLS (triangles), and the calculated strain field (solid line) using a simple continuum model. The residual strain is significantly less than theoretically predicted because of plastic relaxation and radial cracking during sample cooling.

Real-time observation of x-ray fluctuations can provide valuable information about the structural dynamics of a wide range of systems including metallic alloys, glasses, complex fluids, and biological specimens. X-ray photon correlation spectroscopy (or x-ray intensity fluctuation spectroscopy) has been demonstrated to be a promising technique for studying such dynamics. For this type of experiment, an intense highly coherent x-ray beam is required. We tested the setup for a new method of measuring correlated x-ray fluctuations, by x-ray heterodyne correlation spectroscopy, at 2-BM-A in December 1996. In February 1997, we installed and tested it at 2-ID-D. In the first phase of the experiment, we tested the stability of the beam using two collinear pinholes and monochromatic beam (Si (111)). The auto-correlation function of the direct beam intensity passing through the second pinhole was measured, indicating the angular beam stability was better than  $0.5 \mu\text{rad}$ , once a good orbit was established. In the second phase, Fraunhofer diffraction patterns were measured for  $5\text{-}\mu\text{m}$ -diameter pinholes by both scanning a  $5 \mu\text{m}$  analyzing pinhole and using a CCD camera. More than twenty fringes were resolved in the CCD image, indicating high spatial coherence of the beam at the pinhole location and that our pinholes were of high quality. Fraunhofer patterns with good visibility were obtained from pinhole diameters up to  $20 \mu\text{m}$ , indicating that the spatial coherence width of the incident beam was of this scale. Static speckle patterns were then measured from a Vycor glass sample for  $5$ ,  $10$  and  $20 \mu\text{m}$  source pinholes (Fig. 4.58). The speckle size and visibility was found to change accordingly. In the final phase, pink beam was used. The Pt pinhole used proved to be robust for sustaining the pink beam, and optical microscopy showed no damage resulted from the high incident x-ray flux. We



*Fig. 4.58 Speckle pattern from coherent scattering by a porous Vycor glass. The image was captured by a CCD camera at  $1.6 \text{ m}$  using a  $5 \mu\text{m}$  Pt source pinhole.*

are now ready to perform dynamic studies during the next available beam time.

We also demonstrated x-ray fluorescence fluctuation spectroscopy for the first time. This is a novel technique that combines high source brilliance and microfocusing to study number fluctuations as a function of time. Because illumination of a very small volume is required in order to measure the number fluctuation of a specific element in the sample, we used a zone plate to focus the incident beam to  $0.6 \mu\text{m} \times 1 \mu\text{m}$ . We successfully observed the fluctuating fluorescence signal of a gold colloid sample and calculated its auto-correlation function, from which the dynamic information was obtained. Both the translation and rotation diffusion constants were measured. This technique has the virtue of elemental specificity and may find application in studies of material and biological systems.

### ***High resolution spectroscopy***

The 2-ID-C branch line is dedicated to polarization-dependent spectroscopy and instrument development in the intermediate energy range from 0.5 to 3 keV. In order to preserve the beam polarization and to achieve high flux throughput simultaneously at high resolving power, the 2-ID-C branch line uses a grazing incidence SGM. The experiment station offers a UHV experimental chamber with separate analysis and preparation sections. This chamber has a high efficiency electron/ion energy analyzer, LEED system, electron gun with a beam size adjustable to less than 1000 Å, ion sputter gun, thin film evaporation system with piezo thickness monitor, and a precision sample manipulator.

The spectroscopy program includes surface science studies of the magnetic properties of thin films and multilayers containing transition metals and rare earth compounds. A major part of the program is devoted to studying the properties of these structures using angle, spin and spatially resolved photoemission, as well as by resonant scattering. Atoms and simple molecules will be studied both in gas phase, and as surface adsorbates, primarily with the electron/ion analyzer. High detection efficiency of the analyzer will enable resolution of weak nondipole or satellite features. It will also be possible to make correlated electron-electron, electron-ion or electron-photon measurements using coincidence techniques.

### ***Source diagnostics***

As part of SRI-CAT's mission to develop and characterize new sources, we have made considerable progress in 1996 measuring the absolute flux, coherent flux, source size and source divergence of the 3.3-cm-period

undulator A at 2-ID (Cai et al., 1996a, 1996b).

In addition, the spectrum of undulator A was measured for two tapered-gap configurations: (a) upstream gap = 18.5 mm, downstream gap = 19.5 mm; (b) upstream gap = 18.5 mm, downstream gap = 21.5 mm. While the measured spectrum agrees well with that calculated using XOP code (Dejus & Sanchez del Rio, 1996) for the untapered case, the spectra for the tapered cases do show significant discrepancies. We are currently looking into this.

## **2-BM**

The 2-BM scientific program focuses on development of deep x-ray lithography and development of techniques and instrumentation in support of the Sector 2 beamlines.

### ***Optics characterization and technique development***

Also under development at 2-BM are instrumentation, diagnostics, and optical schemes and techniques for high brilliance ID and BM sources, and x-ray optics testing and characterization including reflectivity, scattering, and diffraction measurements on mirrors, multilayers, crystals and gratings, zone plates, and other focusing elements. These capabilities support the Sector 2 scientific programs and enable more efficient utilization of the shared time on the three branch lines of 2-ID.

During commissioning, experiments were conducted in the 2-BM-A station. The FOE is not suitable for some measurements such as

scattering due to the higher background. Other experiments were conducted, and the highlights follow:

- Microtomography experiments using a high spatial resolution CCD camera were performed on microstructures of interest. The data collection of 90 views within a  $180^\circ$  range was completed within half an hour. The reconstruction demonstrated a very high spatial resolution of 1-2  $\mu\text{m}$  in all three directions (Fig. 4.59).
- The focusing efficiency of blazed zone plates with a 3-step profile were measured to be 38-44%. This is considerably higher than the 25% efficiency measured on conventional binary zone plates with a single-step profile. Also, the background intensity

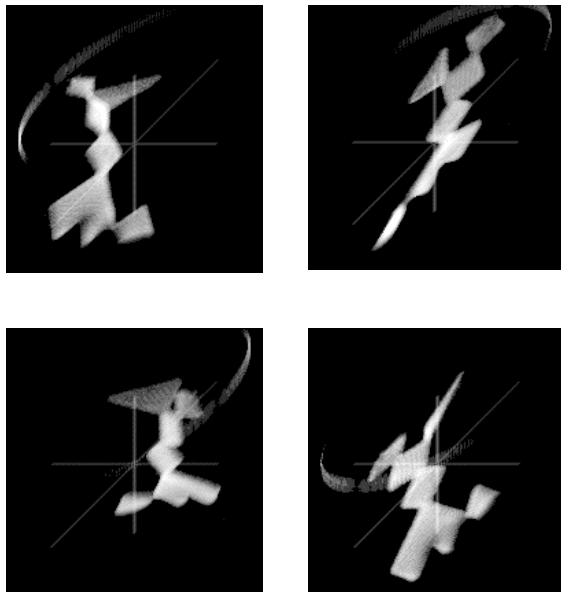


*Fig. 4.59 Reconstruction of a gold microstructure imaged with microtomography. The gold squares are  $100\ \mu\text{m} \times 100\ \mu\text{m} \times 10\ \mu\text{m}$  in size. The snapshots show the bent and twisted shape of the square chain.*

from zero and high orders in the case of blazed zone plates is much suppressed relative to the first order ( $<1:100$ ), which is critical for high sensitivity microanalysis measurements.

- Instrumentation for heterodyne correlation spectroscopy were tested. The feasibility of the concept and the experimental setup were verified. The quality of the entrance pinhole was confirmed by measuring its diffraction effects.
- The reflectivity and scattering from a superpolished Al substrate coated with electroless Ni (intended for x-ray astronomy applications) were measured. These data were compared with AFM and WYCO roughness measurements to assess their validity at a different spatial frequency region.
- The reflectivity of the first mirror was measured, and it agrees with the theoretical reflectivity within 5% from 10 to 35 keV. The reflectivities of several candidate multilayers for the monochromator were measured and the filter foils in the filter assembly were characterized by transmission.

### ***Deep x-ray lithography***

A key objective at 2-BM is to develop deep x-ray lithography (DXRL) at energies above 1 keV. Deep x-ray lithography is uniquely capable of fabricating high precision microstructures with very high aspect ratios (height/lateral dimension) (Ehrfield & Münchmeyer, 1991; Ehrfield &

Lehr, 1994). This technique will be exploited to fabricate diffractive optical elements such as zone plates and gratings, slits and pinholes, and other components such as micro-mechanical parts.

With a high critical energy and a highly collimated beam, the APS is well suited for producing high-aspect-ratio microstructures in thick resist films ( $>1$  mm) using DXRL. The 2-BM beamline was designed to exploit these benefits and to advance the capabilities of DXRL. Initial applications include x-ray optical elements and advanced accelerating structures. The process of fabricating microstructures using DXRL is shown schematically in Fig. 4.60. The x-ray mask consists of patterns defined by an absorbing material (usually Au) supported on a thin plate (Be, Si, etc.). The pattern is then transferred to the resist layer using x-ray proximity exposure. A widely used photoresist is

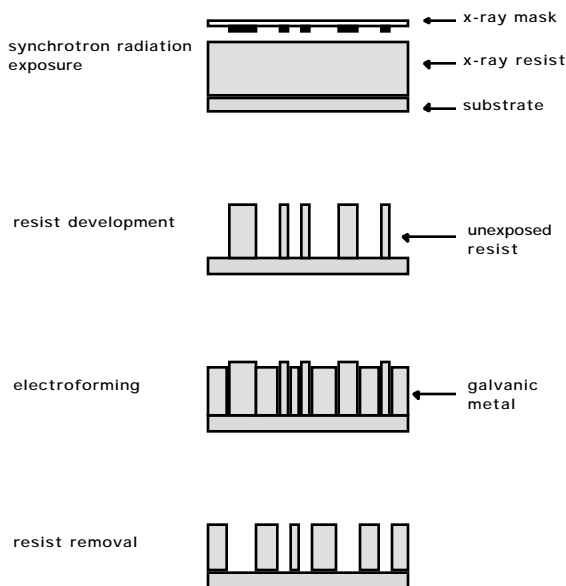


*Fig. 4.60 Schematic of the DXRL process: exposure, resist development, electroforming, and resist stripping. Note the final structure has a higher aspect ratio than the mask.*

polymethylmethacrylate (PMMA). To obtain a uniform exposure, the mask and resist are scanned together through the x-ray beam in the vertical plane. After exposure, the resist is developed in organic solvent, the final structures are electroformed onto the substrate, and the remaining resist is stripped away. This pattern transfer process is highly precise, and the aspect ratio of the final structure can be considerably enhanced relative to the original mask.

Lithography exposures had been performed in the FOE, using a prototype scanner developed for use during the initial phase. Using this scanner, initial characterization of 1- and 2.5-mm-thick PMMA resists at different x-ray spectra, dose rate, total dose, and developer conditions was performed. A more advanced scanner that can better utilize the source characteristics and enables exposures of inclined or nonplanar structures has been designed and specified. An EPICS-based exposure control module has been developed to integrate the scanner operation with other beamline controls and to automate the exposure.

Beryllium is a promising substrate material for the x-ray mask, providing better mechanical stability and thermal conductivity than silicon, which is critical for handling the high thermal load at the APS. Beryllium masks with patterned gold structures were fabricated, and their radiation stability in the x-ray beam was studied. Figure 4.61 shows structures in a developed 1-mm-thick PMMA resist exposed with the beryllium mask. The patterns are part of a prototype coded aperture for x-ray astronomy application, fabricated in collaboration with NASA Goddard Space Flight Center. Also, fabrication and initial exposure for mm-wave accelerating cavity structures have been done together with the APS/ASD rf group.





*Fig. 4.61 Scanning electron micrograph of structures of coded aperture patterns in a 1-mm-thick PMMA resist.*

### Future R&D Plans

The 2-BM beamline will be completed in late 1997 with the installation of a collimating mirror, multilayer monochromator for broad bandpass experiments, and a 6-circle diffractometer for microdiffraction applications. The mirror will provide a collimated beam with uniform intensity, which will enable us to fabricate more precise microstructures and provide better spatial resolution in microfocusing applications. A microfocusing setup will also be installed in the experiment station. Two enhancements will be added to the lithography scanner: a sample rotation stage for fabricating conical structures, and an interferometric feedback system. A mask-to-substrate aligner will be developed and integrated with the scanner to enable precise field stitching and multiple step exposure. A processing cleanroom will be built to provide mask fabrication, resist processing, electroforming, and sample metrology capabilities.

Final commissioning activities at 2-ID-B will include installation and characterization of a real-time BPM system. Deep multilayer gratings, which offer substantially higher

efficiency, will be fabricated and tested in the 2-ID-B monochromator. A high-harmonic-rejection and beam steering system based on a double-bounce mirror will also be developed to attenuate high undulator harmonics passed by the monochromator. The 2-ID-B scanning microscope software will be enhanced, enabling XANES imaging, microtomography, microfluorescence, and microdiffraction experiments. We will explore possibilities for real-time microtomography using both high performance workstations and an on-site teraflop supercomputer.

The UHV photoemission station at 2-ID-C will be used for surface science, gas phase, thin film and multilayer measurements. The UHV goniometer will be used for polarization-dependent studies of thin films and multilayers using plane polarized radiation. We will also develop a zone-plate-based microprobe system and CCD detector for photoemission and fluorescence spectromicroscopy with both systems. A mini-Mott electron spin polarimeter will be commissioned and used for photoemission measurements of magnetic samples. Several external SRI-CAT members will use their own experimental equipment at 2-ID-C, e.g., an angle-resolving photoemission station for photoelectron holography (T.-C. Chiang, University of Illinois), and energy dispersive secondary emission fluorescence analyzer (Dave Ederer, Tulane University).

At 2-ID-D/E, a 13-element detector, wavelength dispersive spectrometer, large-format CCD camera, and precision conical slits will be added to the instrumentation supporting the hard x-ray microscope. Further integration of the microscope software and hardware will be completed for routine operation of the system by general users. In support of the high resolution x-ray optics development program, a high speed sputtering system for producing

zone plates for high energy (40-150 keV) applications will be designed and procured. Related instruments, such as a polisher, slicer, and laser system for accurately measuring the diameter of sputtered-slice zone plates, will be developed.

Because of the long lead times required for manufacturing x-ray mirrors, we will begin development of a high heat load x-ray mirror for operation with 300 mA current in the storage ring. This mirror will replace the high heat load mirror (M1) currently used in our beamline.

We are developing a new technique for microfocusing x-ray beams from a high brilliance source using thin-film waveguides. The method consists of using the evanescent wave produced in a thin cover plate for the waveguide (designed for total reflection of the incident beam) to excite a resonant mode in the guide, thereby coupling most of the incident beam intensity into the region between the plane surfaces of the waveguide, which can be microfabricated to be as small as 20 nm. The method has already been demonstrated by us previously in a preliminary experiment at the ESRF (Feng et al., 1995). The technique will also be used to study the structure and dynamics of fluids placed inside the waveguide.

We are also developing a technique for measuring residual stress in components machined of materials ranging from Be to U, using the microdiffraction capabilities of the instrumentation at station 2-ID-D/E, and the capability of microfocusing x-ray beams with energies over 100 keV currently under development. The method should yield a 3-D map of the texture and strain in the sample, and could be used, for instance, to image the stress distribution around a crack tip.

#### 4.4.4 Sector 3

The Sector 3-ID beamline is dedicated to high energy resolution x-ray scattering studies in the energy range of 6-30 keV, with a energy bandpass of  $10^{-5} < E/E < 10^{-13}$  eV. The development of optical components in terms of monochromators, analyzers, and detectors is heavily emphasized in the early years of operation. Along these lines, novel monochromator concepts are being introduced and tested.

The 3-ID beamline was optimized for the inelastic x-ray scattering and nuclear resonant scattering programs. The 5-meter-long straight section for the beamline has room for two IDs that can be alternatively operated. Currently, a special 2.7-cm-period undulator, optimized for peak brilliance around 14 keV is installed, with the option of adding undulator A when energies out of the range of the 2.7-cm-period undulator are required. The layout of this undulator beamline is given in Fig. 4.62. The FOE, 3-ID-A, covers the area of the beamline immediately downstream of the ratchet-wall penetration and is used to house various components that manipulate the x-ray beam prior to transmitting the beam downstream to the experiment stations. The components in 3-ID-A are permanent parts of the beamline and include filters, white-beam slits, the Kohzu DCM, monochromatic-beam shutters, and a bremsstrahlung collimator/stop. A beryllium window separates the monochromator from the FE (i.e., the beamline inside the ratchet wall) and, hence, the storage-ring vacuum. The 3-ID-B station is located directly downstream of 3-ID-A and houses the mirror and high resolution optics.

The high resolution monochromator consists of two high angular resolution stages (12.5 nanoradians/step) attached to vertical

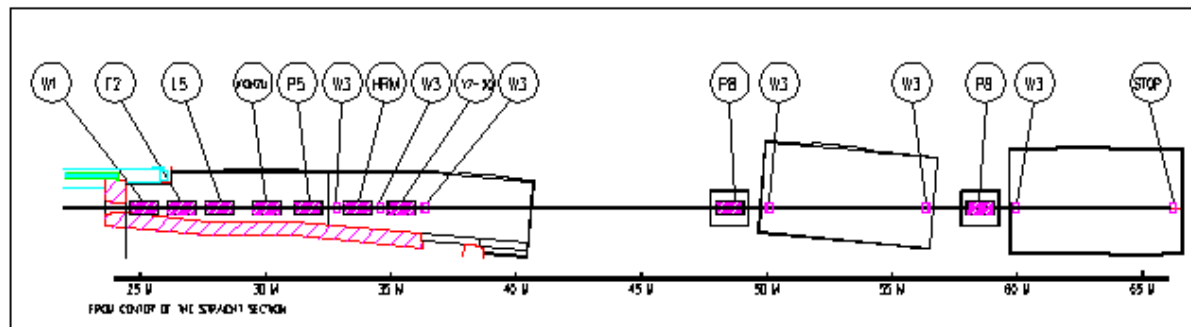


Fig. 4.62 Schematic layout of Sector 3-ID. W1 and W3: beryllium windows, F2: filter, L5: white-beam slits, KOHZU: double-crystal high heat load monochromator, P5: white-beam stop, and monochromatic-beam shutter, HRM: high resolution monochromator (Kohzu), Y7-30: double-groove mirror (Zeiss), P8: monochromatic-beam shutter

stages with 1  $\mu\text{m}/\text{step}$  resolution. This system was custom built by Kohzu-Seiki Co., Japan (Model No: AAG-100). The flexibility of this system allows us to use both 4-bounce nested crystal geometry, as well as 2-bounce flat crystal geometry. The available set of monochromators are tabulated in Table 4.11.

The mirror is a novel design two-groove system on the same block with dual purposes: collimation and focusing. The cylindrical grooves can be bent pneumatically to a toroidal shape. The 80-cm-long zerodur mirror is coated with Pd to operate at a fixed angle of 2 mrad. The UHV-compatible system is contained with two Be windows on each end. The mirror and the bending mechanism are built by Zeiss, Germany.

Station 3-ID-C is dedicated to inelastic x-ray scattering using backscattering crystal analyzers. There is a Huber diffractometer with a 2.6-m-long arm suitable to mount the analyzer. In addition, there are facilities for low temperature and an optical table.

Station 3-ID-D is dedicated to nuclear resonant scattering studies. It is equipped with an optical table, a 6-circle Huber goniometer, liquid He cryostat with reversible 7 T superconducting magnet, high-precision stages, and nanosecond timing electronics. Table 4.12 lists the characteristics and equipment associated with the 3-ID beamline.

### Current Status

We commissioned the first two stations of this beamline in 1996. We have achieved a count rate of  $1.2 \times 10^{13}$  photons/sec/eV/100 mA at 14 keV in the first harmonic of the undulator. The beam size is 0.8 mm by 2 mm at 35 m away from the source. Stations 3-ID C and 3-ID-D are scheduled to be commissioned in the April-June 1997 period. We also have plans to replace the liquid-gallium-cooled monochromator with either water-cooled diamond or liquid-nitrogen-cooled Si, after testing the performance of both systems.

**Table 4.11 High Energy Resolution Monochromators Available at 3-ID**

	Energy (keV)	Bragg Reflections	Energy Resolution (meV)	Angular Acceptance ( $\mu$ rad)	Purpose
1.	8.4	Si (333) - (444) channel-cut pair	15	29	Nested monochromator <sup>a</sup> for $^{169}\text{Tm}$ nuclear resonance
2.	8.4	Si (333) - (333) channel-cut pair	N/A	44	Polarizer/Analyzer <sup>b</sup> for $^{169}\text{Tm}$ nuclear resonance. Polarization rejection ratio: $10^{-8}$
3.	13.841	Si (440) - (844) channel-cut pair	5	20	Nested monochromator for inelastic x-ray scattering with Si (777) analyzer
4.	14.413	Si (422) - (1064) channel-cut pair	5.5	22	Nested monochromator for $^{57}\text{Fe}$ nuclear resonance
5.	14.413	Si (975) - (975) flat crystals	0.9	8.4	2-bounce monochromator <sup>c</sup> for $^{57}\text{Fe}$ nuclear resonance
6.	14.413	Si (975) - (975) flat crystals	0.66	12	2-bounce monochromator <sup>c</sup> for $^{57}\text{Fe}$ nuclear resonance
7.	14.413	Si (840) - (840) channel cut pair	N/A	10	Polarizer/Analyzer for $^{57}\text{Fe}$ nuclear resonance. Polarization rejection ratio: $10^{-8}$
8.	21.5	Si (440), (15 11 3) flat crystals	1	12	2-bounce monochromator for $^{151}\text{Eu}$ nuclear resonance
9.	23.87	Si (400) (12 12 12) flat crystals	4.8	15	2-bounce monochromator for $^{119}\text{Sn}$ nuclear resonance
10.	23.87	Si (333) - (555) channel-cut pair	23	7	Nested monochromator for $^{119}\text{Sn}$ nuclear resonance

<sup>a</sup> Nested monochromator refers to an arrangement of a higher order reflection channel-cut crystal nested into a lower order reflection channel cut crystal. The function of the lower order asymmetrically cut crystal is to increase the angular acceptance of the monochromator, while the higher order reflection crystals bring the energy bandpass down. The design and operational principles of nested monochromators are described in (1) T. Ishikawa, Rev. Sci. Instr. 63 (1992) 1015 (1992); (2) T. Toellner, SPIE proceedings, vol. 1740 (1992) 218. (1992); and (3) T. Mooney, Nucl. Instr. Meth. A347 (1994) 348.

<sup>b</sup> Polarizer/analyzer refers to an arrangement in which the channel cut crystals have Bragg angle close to  $45^\circ$ , satisfying the necessary condition for an effective polarization selection by providing a large angular acceptance, for one component of linear polarization while suppressing the other component and high reflectivity. By placing the polarizer and analyzer at  $90^\circ$  with respect to each other, it is possible to measure any change in the state of polarization of the beam when it travels through an optically active medium. The details are described in T. Toellner, Appl. Phys. Lett. 67 (1995) 1993.

<sup>c</sup> 2-bounce flat crystals refer to a relatively new arrangement in which very high order reflection crystals with extreme asymmetric cuts are placed in dispersive geometry to minimize the energy bandpass while maintaining a reasonable angular acceptance. The details of these monochromators can be found in T. Toellner, Ph.D. Thesis, Northwestern University (1996), A. Chumakov, Nucl. Instr. Meth. A383 (1996) 642.



## High resolution optics

Our highest priority was to improve the energy resolution of the monochromators. Along these lines we have tested three classes of monochromators:

- Nested monochromators (4-bounce)
- Flat crystals (2-bounce)
- Polarizer/analyzers as monochromators

We have built two sets of nested monochromators to work at 14.4 keV for nuclear resonant scattering studies and at 13.8 keV for inelastic x-ray scattering coupled to a Si (777) backscattering analyzer. The energy resolution is 5 meV, and the flux achieved is  $2 \times 10^9$  Hz in this bandpass.

In order to reduce the energy bandpass further, we have prepared high order Bragg reflection crystals with asymmetry angles close to the Bragg angle. The first crystal, for example, is a Si (975) with a Bragg angle of 80.4 degrees, and it is asymmetrically cut with  $b=1/22.3$ , and the second crystal with  $b=10.4$ . This crystal pair has an angular acceptance of 8.5  $\mu$ rad. When the asymmetry angles are changed such that  $b=1/38$  for the first crystal and  $b=22.3$  for the second crystal, the energy bandpass is further reduced to 0.66 meV, while the angular acceptance is increased to 11  $\mu$ rad. The measured flux is 0.4 GHz at 0.9 meV ( $E/E=5.7 \times 10^{-8}$ ), and 0.2 GHz at 0.66 meV resolution ( $E/E=4.5 \times 10^{-8}$ ). This represents 4% efficiency, while the theoretical limit is about 10%. The energy resolution, measured using coherent nuclear forward scattering, is shown in Fig. 4.63b, along with phonon density of states measured via inelastic nuclear resonant scattering,

Fig. 4.63a. These monochromators are the first instruments suitable to measure lattice excitations with sub-meV resolution using x-rays.

Bragg reflections near  $45^\circ$  act as x-ray polarizers. With the availability of undulator sources, the same type of crystals can be used as analyzers. Such a pair has been used to generate a monochromatic beam with an energy bandpass of 0.8  $\mu$ eV with about  $10^4$  Hz flux. The angular acceptance of Si (8 4 0) reflection is 10.2  $\mu$ rad when the asymmetry angle is  $-43^\circ$  for a Bragg angle of  $45.1^\circ$ . This should be compared to the  $15 \times 52 \mu$ rad vertical and horizontal divergence of undulator radiation. This discrepancy may be remedied when the collimating branch of the mirror is operational. The polarization switching was provided with an iron thin film in grazing-incidence geometry, with a magnetic field applied along the incident beam.

## Vibrational dynamics of thin films

The high energy resolution (meV) inelastic neutron and x-ray scattering studies have been limited to bulk materials. This is partly due to the high penetration of neutrons, as well as the lower brightness of neutron sources. In the case of conventional inelastic x-ray scattering, the scattering from the sample has to originate from a small spot size to lend itself to energy analysis with meV resolution, thus precluding grazing-incidence geometry where the beam is spread over a large area. These obstacles have been overcome in case of inelastic nuclear resonant scattering under grazing-incidence geometry. By enhancing the electric field amplitude in the region where the thin film is deposited, it is possible to increase the signal

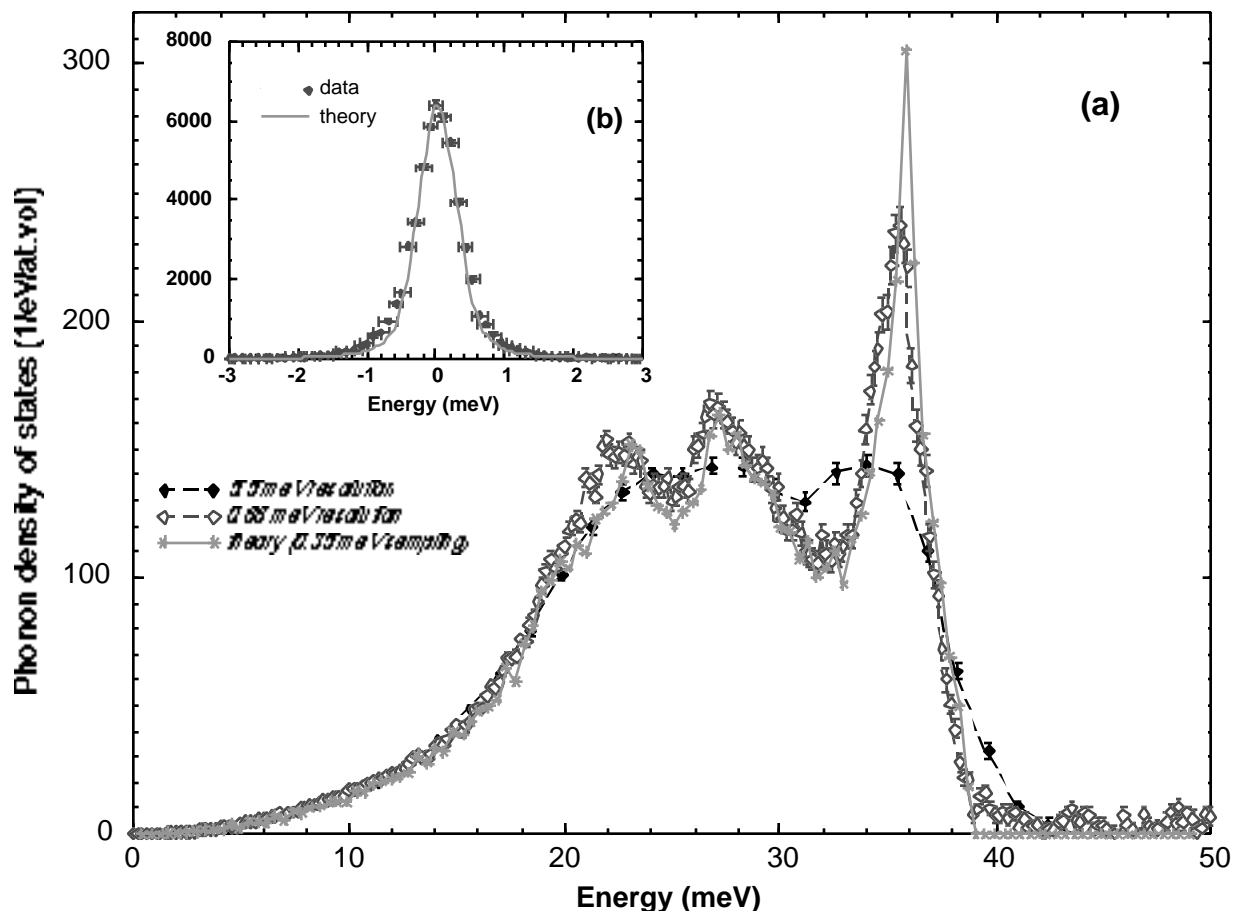


Fig. 4.63 (a) The photon density of states of iron measured by inelastic nuclear resonant scattering. The black filled circles were measured with the 5.5-meV nested monochromator, while the empty circles were measured with 0.66-meV-resolution, 2-bounce flat crystals. The theory curve was calculated from experimentally determined force constants via fitting the coherent neutron scattering data. (b) The inset shows the resolution function of the 0.66 meV monochromator as measured with coherent nuclear forward scattering. The theoretical calculation includes the brilliance function of the incident beam coupled to the dynamical diffraction equations.

similar to the bulk values. This increase in the inelastic fluorescence yield is shown in the Fig. 4.64 at 4 mrad. The incident beam energy was set at 20 meV above the nuclear resonance energy. This technique is applied to  $\text{Fe}_{1-x}\text{Tb}_x$  amorphous thin films with a thickness of 175 Å. A series of samples are measured as a function of  $x$ , and in addition to phonon density of states (Fig. 4.65a), force constants are derived from the third moment of the phonon spectrum (Fig. 4.65b).

### Phonon density of states measurements of iron and iron oxides

The direct measurement of phonon density of states with sub-meV resolution using x-rays has been elusive, because neither monochromatization nor analysis has been trivial. By using nuclear resonance as an analyzer, the energy gain or loss of a photon during

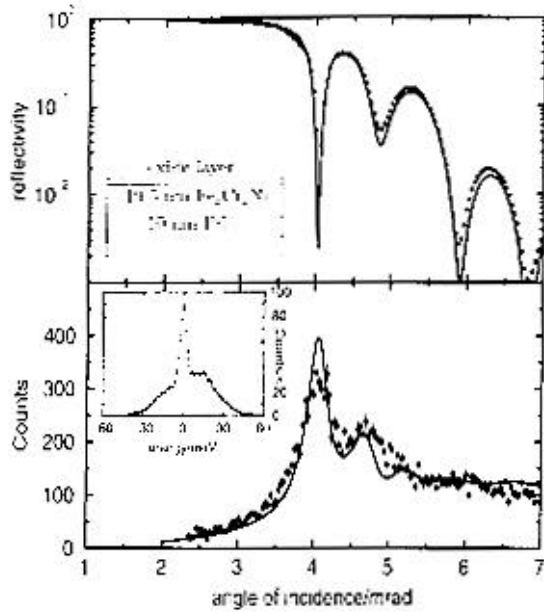


Fig. 4.64 The principle of phonon density of states measurements of thin films: (Top) The electronic reflectivity of  $\text{Fe}_2\text{Cr}_2\text{Ni}$  film as a function of incidence angle. The sharp drop at 4 mrad corresponds to a cancellation of the total external reflected beam at the grazing incidence anti-reflection point. (Bottom) The delayed fluorescence yield as a result of nuclear decay, whose excitation is caused by phonon creation at +20 meV above the nuclear resonance energy. The enhanced yield at 4 mrad is caused by the increase in electric field amplitude in the film due to total external reflection from the Pd layer, and it coincides with the drop in reflectivity at the grazing incidence anti-reflection point. (Inset) The inelastic nuclear scattering data obtained as a function of incidence energy. A 5.5-meV-resolution nested monochromator was used in this experiment. The negative energies correspond to phonon annihilation, while the positive energies correspond to phonon creation.

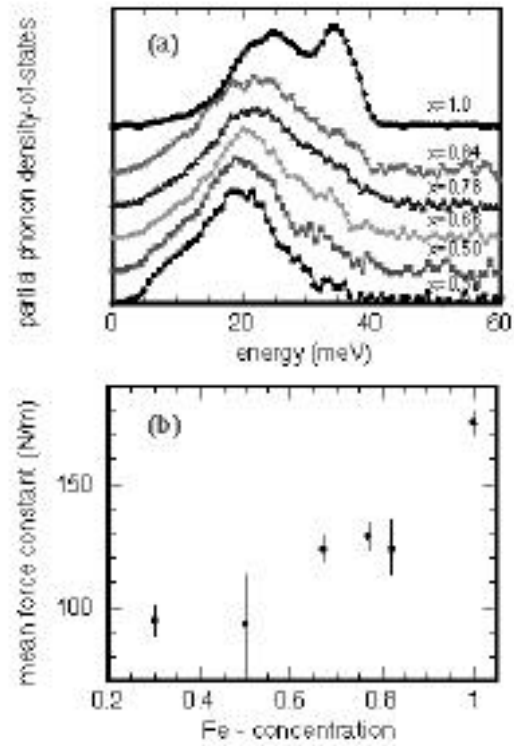


Fig. 4.65 (a) Phonon density of states of a  $\text{Fe}_{1-x}\text{Tb}_x$  system, as a function of  $x$ . (b) The force constants derived from the third moment of phonon creation-annihilation spectra as a function of  $x$ . Such measurements with thin films are facilitated by employing grazing-incidence geometry and nuclear resonance as an analyzer to measure lattice excitations.

interaction with lattice excitations can be measured, as shown in Fig. 4.66a. It is possible to extract phonon density of states (Fig. 4.66b). Using the 0.66 meV monochromator, the phonon density of states of iron metal and various iron oxides has been measured.

### Test of backscattering analyzers

The energy resolution of several backscattering analyzers has been measured. We have reached an energy resolution of 9 meV



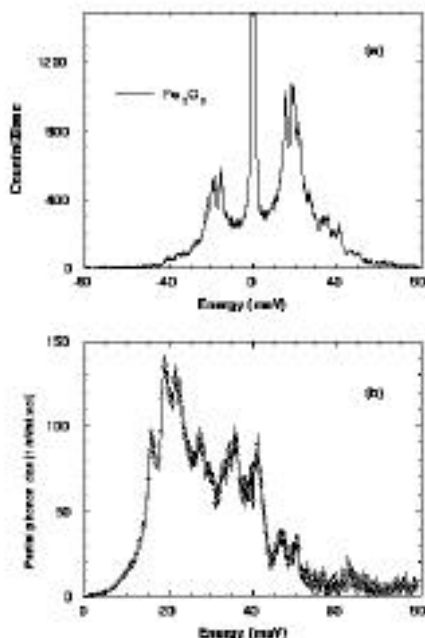


Fig. 4.66 (a) The inelastic nuclear resonant scattering yield as a function of incidence energy for a hematite sample, using 0.66-meV-resolution, two-bounce flat crystals as a monochromator. (b) The phonon density of states derived from the data in (a) indicates many sharp singularities, corresponding to low dispersion points in optical, and perhaps, acoustical phonons.

at 13.842 keV. This analyzer, coupled with an in-line nested monochromator with 5-meV bandpass, was used to study a particular optical branch in diamond to verify a maximum in the phonon dispersion curve (see Fig. 4.67). This set of measurements has demonstrated the advantage of scanning monochromator by changing the angle, rather than the temperature.

#### 4.4.5 New R&D Initiatives

The primary new initiative for SRI-CAT is the development of an ID beamline in Sector 4.

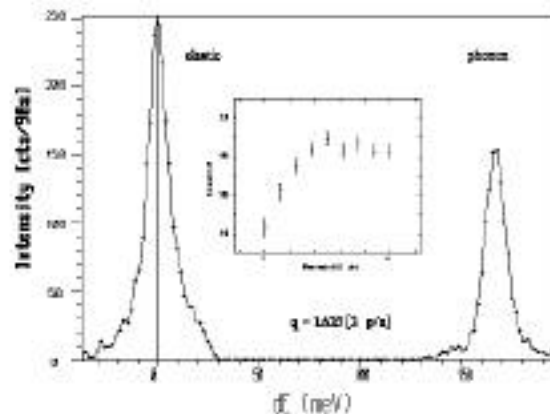


Fig. 4.67 Observation of the longitudinal optical phonon along the  $\langle 100 \rangle$  direction in diamond. This has been achieved by using a nested 4-bounce monochromator with 5-meV resolution and a Si (777) backscattering analyzer, giving a total resolution of 12 meV. The inset shows the dispersion of this mode as a function of momentum transfer.

The unique feature of this beamline will be the availability of x-rays with variable polarization from 0.5 keV to 100 keV and higher. This will be accomplished in the low energy range (0.5 keV to 5 keV) with a helical undulator and with crystal optics and with APS undulator A for energies above 5 keV. These unique tunable polarization and energy capabilities, located on one beamline, will provide scientists with the ability to cover all important absorption edges from M to K for magnetic spectroscopy experiments and resonant magnetic scattering.